Plasma cell but not CD20-mediated B-cell depletion protects from bleomycin-induced lung fibrosis

Cecilia M. Prêle[1,2,12], Tylah Miles[1,12], David R. Pearce[3], Robert J. O'Donoghue[4], Chris Grainge[5,6], Lucy Barrett[1], Kimberly Birnie[1], Andrew D. Lucas[1], Svetlana Baltic[1], Matthias Ernst[7], Catherine Rinaldi[8], Geoffrey J. Laurent[1,2], Darryl A. Knight[9], Mark Fear[1,10], Gerard Hoyne[1,11], Robin J. McAnulty[3,13] and Steven E. Mutsaers[1,2,13]

[1]Institute for Respiratory Health, The University of Western Australia, Nedlands, Australia. [2]Centre for Cell Therapy and Regenerative Medicine, School of Biomedical Sciences, The University of Western Australia, Nedlands, Australia. [3]Centre for Inflammation and Tissue Repair, Division of Medicine, University College London, London, UK. [4]Department of Pharmacology and Therapeutics, University of Melbourne, Melbourne, Australia. [5]Centre for Healthy Lungs, Hunter Medical Research Institute, University of Newcastle, Newcastle, Australia. [6]Department of Respiratory and Sleep Medicine, John Hunter Hospital, Newcastle, Australia. [7]Olivia Newton John Cancer Research Institute and La Trobe University School of Cancer Medicine, Heidelberg, Australia. [8]Centre for Microscopy Characterisation and Analysis, The University of Western Australia, Nedlands, Australia. [9]Providence Health Care Research Institute, Vancouver, BC, Canada. [10]Burn Injury Research Unit, School of Biomedical Sciences, The University of Western Australia, Nedlands, Australia. [11]The University of Notre Dame Australia, Fremantle, Australia. [12]C.M. Prêle and T. Miles have contributed equally to this work and share first authorship. [13]S.E. Mutsaers and R.J. McAnulty have contributed equally to this work and share senior authorship.

Corresponding author: Steven E. Mutsaers (steven.mutsaers@uwa.edu.au)

Shareable abstract (@ERSpublications)
Bortezomib-mediated depletion of plasma cells but not anti-CD20-mediated B-cell depletion inhibited bleomycin-induced lung fibrosis, suggesting that plasma cells are a therapeutic target for fibrotic lung disease such as IPF. https://bit.ly/3Nv4w5P

Cite this article as: Prêle CM, Miles T, Pearce DR, *et al*. Plasma cell but not CD20-mediated B-cell depletion protects from bleomycin-induced lung fibrosis. *Eur Respir J* 2022; 60: 2101469 [DOI: 10.1183/13993003.01469-2021].

This article has an editorial commentary: https://doi.org/10.1183/13993003.01748-2021

Received: 30 May 2021
Accepted: 16 May 2022

Abstract

Idiopathic pulmonary fibrosis (IPF) is an interstitial lung disease associated with chronic inflammation and tissue remodelling leading to fibrosis, reduced pulmonary function, respiratory failure and death. Bleomycin (Blm)-induced lung fibrosis in mice replicates several clinical features of human IPF, including prominent lymphoid aggregates of predominantly B-cells that accumulate in the lung adjacent to areas of active fibrosis. We have shown previously a requirement for B-cells in the development of Blm-induced lung fibrosis in mice. To determine the therapeutic potential of inhibiting B-cell function in pulmonary fibrosis, we examined the effects of anti-CD20 B-cell ablation therapy to selectively remove mature B-cells from the immune system and inhibit Blm-induced lung fibrosis. Anti-CD20 B-cell ablation did not reduce fibrosis in this model; however, immune phenotyping of peripheral blood and lung resident cells revealed that anti-CD20-treated mice retained a high frequency of $CD19^+$ $CD138^+$ plasma cells. Interestingly, high levels of $CD138^+$ cells were also identified in the lung tissue of patients with IPF, consistent with the mouse model. Treatment of mice with bortezomib, which depletes plasma cells, reduced the level of Blm-induced lung fibrosis, implicating plasma cells as important effector cells in the development and progression of pulmonary fibrosis.

Introduction

Idiopathic pulmonary fibrosis (IPF) is an aggressive interstitial lung disease (ILD) characterised by excessive extracellular matrix deposition and a chronic, progressive decline in lung function leading to death [1]. Recent advances from genome-wide association studies have highlighted the significant role of epithelial dysfunction in the pathogenesis of IPF; however, there remain limited treatment options with minimal impact on survival time for IPF patients [2]. While several loci associated with epithelial function, including *MUC5B*, *TERT* and *TERC*, are thought to underpin the development of IPF [3], the variable

progression of disease between patients with identical gene variants illustrates the complexity of IPF pathogenesis.

There is growing evidence that suggests a significant role for immune cells in the pathogenesis of IPF [4, 5]. Lung tissue of IPF patients often display prominent lymphoid aggregates composed of T-cells, B-cells, macrophages and dendritic cells [6, 7]. A subset of IPF patients present with serum autoantibodies, suggesting a breakdown in immune tolerance to either systemic (*e.g.* DNA or RNA) or lung-specific autoantigens that may be derived from damaged or dying lung epithelial cells [8–11]. Fibrosis is not unique to IPF, as it is observed in a range of other connective tissue diseases including systemic lupus erythematosus (SLE), systemic sclerosis (SSc), Sjogren syndrome and rheumatoid arthritis [12]. These diseases share similar immune pathologies with IPF [13–15], suggesting that a breakdown in immune regulation plays an important role in the pathogenesis of lung fibrosis [7, 16, 17].

Mature B-cells normally reside within lymphoid follicles of secondary lymphoid organs where they coordinate antibody synthesis in response to antigen [18]. Several different B-cell subsets exist within the immune system including naïve and memory cells and effector cells that can be short-lived antibody-secreting plasmablasts or long lived-plasma cells [19, 20]. Long-lived plasma cells are now thought to hone to specific areas of the bone marrow, producing low levels of antibody for an indeterminate period of time and ramping up production if they encounter antigen, in addition to the rapid reactivation of memory B-cells in the spleen and lymph nodes that can recirculate in peripheral blood [21]. Plasma cells are derived from activated, proliferating B-cells [22], typically requiring B-cell receptor (BCR) stimulation and signals from $CD4^+$ T-helper cells in a T-cell dependent immune response, or BCR with Toll-like receptor stimulation plus cytokines from accessory cells in T-cell independent responses [23, 24].

Two additional B-cell populations are B1-cells which localise to the peritoneal and pleural cavities, and marginal-zone B-cells (MZB) of the spleen. Both these B-cell populations display innate-like properties that produce low-affinity "natural" IgM antibodies against microbial antigens [25, 26]. B1-cells are important for regulating tissue homeostasis through the recognition and clearance of apoptotic cells that can express self-antigens [27]. A failure to clear cellular debris or dying cells can potentially drive inflammation and autoimmunity [28]. B- and T-cells can also be recruited to peripheral tissues in response to infection or chronic immune stimulation, where they form tertiary lymphoid structures. These aggregates are organised similar to secondary lymphoid tissues consisting of B-cell follicles, in which germinal centres can develop, and T-cell areas that harbour antigen-presenting cells [29].

We have demonstrated that in bleomycin (Blm)-induced pulmonary fibrosis, B-cell-dominant foci develop in the fibrotic lung tissue within 28 days [5, 30] and that mice lacking T- and B-cells or mature B-cells only were both protected from Blm-induced lung fibrosis [30, 31]. However, these studies did not identify the B-cell subset(s) that may be involved in this process.

In this study we provide evidence that in both mice and humans, $CD20^+$ B-cells accumulate in prominent foci in the lung adjacent to areas of tissue fibrosis. However, depletion of $CD20^+$ B-cells failed to protect mice from Blm-induced pulmonary fibrosis. Importantly, $CD19^+$ $CD138^+$ plasma cells accumulated in significant numbers within the fibrotic lung which were not significantly affected by anti-CD20 antibody treatment. Furthermore, we identified a subset of IPF patients with a high proportion of plasmablasts in the blood and plasma cells in lung tissue, which were localised to discrete foci adjacent to fibrotic tissue. Depletion of lung plasma cells in mice using bortezomib significantly reduced the level of Blm-induced lung fibrosis. Our findings that both IPF and fibrotic mouse lung share similarities in the types of immune cell subsets that aggregate within the lung, and that plasma cell ablation significantly inhibits Blm-induced lung fibrosis, suggest that plasma cells play a significant role in the pathogenesis of lung fibrosis and are a target for ablation therapy

Materials and methods

Bleomycin-induced lung fibrosis

Mouse studies were approved by the University of Western Australia animal ethics committee (RA/3/100/1339 and RA/3/100/1722), Austin Health Animal Ethics Committee (ethics approval identifier 2015-05305 and 2016-05320) and University College London Animal Care Committee under Home Office licence in accordance with the United Kingdom Animals (Scientific Procedures) Act 1986. Male 10–12-week wild-type (wt) C57Bl/6J mice were used in this study. Bleomycin sulphate (Blm) (Hospira, Melbourne, VIC, Australia) or saline (0.9%; Baxter, Old Toongabbie, NSW, Australia) was administered oropharyngeally (1 $mg \cdot kg^{-1}$) unless otherwise stated. Blm-induced weight loss occurred in all animals,

with ⩽10% euthanised as they reached the 20% weight loss ethical limit. A minimum of four animals per group were used for end-point quantitative analysis.

Anti-CD20 B-cell depletion

Anti-CD20 antibody (donated by Genentech, South San Francisco, CA, USA) or isotype control IgG2a (5 mg·kg^{-1}; Cat#02-6200; Thermo Fisher Scientific, Scoresby, VIC, Australia) were administered intraperitoneally either 7 days before and 7 days after Blm treatment (prophylactic treatment) or on days 10 and 19 post-Blm treatment (therapeutic treatment). Blood, spleen and lung tissue samples were collected for cell isolation (supplementary methods) and flow cytometric analysis (supplementary methods) performed using a B-cell flow cytometry antibody screening panel (supplementary table S1): mature follicular B-cells (CD45.2$^+$CD19$^+$CD20$^+$), B1 regulatory B-cells (CD45.2$^+$CD5$^+$CD19$^+$), plasma cells (CD45.2$^+$CD19$^+$CD38$^+$CD138$^+$) and plasmablasts (CD45.2$^+$CD19$^+$CD20$^+$CD138$^-$CD43$^+$CD38$^+$CD27$^+$). In addition, lung tissue samples were weighed and snap-frozen for high-performance liquid chromatography (HPLC) analysis of hydroxyproline [30]. For histological analysis, lungs were inflated and fixed in 4% paraformaldehyde (PFA) and processed for paraffin embedding. Tissue sections (3–5 µm) were stained with Masson's trichrome or Martius scarlet blue using a Tissue-Tek DRS autostainer (Sakura, Japan) and slides scanned on a NanoZoomer HT slide scanner (Hamamatsu, Japan) and images exported with NDP.View2.

Bortezomib plasma cell depletion

Bortezomib stock solutions were prepared at 12.5 mg·mL^{-1} in dimethyl sulfoxide (DMSO) and stored at −80°C in single-use aliquots. Bortezomib was prepared immediately prior to injection and administered at 1 mg·kg^{-1} in 2% DMSO, 30% polyethylene glycol (PEG)300 i.p. twice a week beginning 7 days before Blm treatment (day −7) until day 28 post-Blm treatment. Vehicle only (2% DMSO, 30% PEG300) was administered i.p. to control animals. Blm (2 mg·kg^{-1}), was administered intranasally on day 0. The mice were euthanised 28 days later and lungs inflated and fixed for *ex vivo* micro-computed tomography (µCT) quantification of fibrosis.

Ex vivo *µCT analysis of lung fibrosis*

Lungs were inflated and fixed with 4% PFA, dried with hexamethyldisilazane (Alfa Aesar, Ward Hill, MA, USA) and CT-scanned using a SkyScan 1172 (Bruker-MicroCT, Kontich, Belgium) with 12.6 µm pixel size, as described previously [32]. Reconstructed images were segmented with InForm image analysis software (Perkin-Elmer, Waltham, MA, USA) to exclude background and to segment lungs into normal (green), fibrotic (blue) and airway regions. Data are either represented as percentage volume of fibrosis or sum pixel intensity, as a measure of lung density.

HPLC quantification of lung collagen

Following µCT or snap-freezing, lung tissue was hydrolysed in 6 M hydrochloric acid, amino acids purified and derivitised with 7-chloro-4-nitrobenzo-oxao-1,3-diazole (NBD-Cl; Acros Organics, Geel, Belgium) and hydroxyproline levels measured by reverse-phase HPLC (1100, LiChrospher column; Agilent Technologies, Santa Clara, CA, USA) as described previously [33]. Hydroxyproline content was quantified against a known standard and pro-collagen content of samples calculated.

Histochemical and immunohistochemical analysis of fibrosis and immune cell infiltration in tissue

The expression and distribution of the T-cell marker CD3, mouse pan B-cell marker B220, B-cell marker CD19, plasma cell, B-cell precursor and some epithelial cell marker CD138 (syndecan-1; expresses weak epithelial cell staining) and B1α-cell and T-cell marker CD5 on cells within lung and spleen tissue was determined by immunohistochemistry following a heat-based citrate buffer method of antigen retrieval, as described previously [30]. A minimum of three tissue sections from different levels of the lung in at least three animals were examined for each study. For some immunohistochemistry studies, serial sections were prepared from area of lung examined.

IPF patient samples and age-matched controls

Serum samples from IPF patients (n=20, male=14; mean age 72.6±7.0 years, median age 73 years) and age-matched controls (n=17, male=10; mean age 66.2±9.4 years, median age 66 years) were collected in accordance with National Health and Medical Research Council guidelines and with ethics approval (Belberry application number HREC2011-10-497). Analysis of B-cell activating factor (BAFF), APRIL and CXCL13 levels in IPF and control serum was performed using ProcartaPlex kits (Jomar Life Research, Scoresby, VIC, Australia) and measured on the Luminex 200 (R&D systems, Minneapolis, MN, USA). White blood cells collected from IPF (n=54, male=15; mean age 73.1±6.7 years, median age 73 years) and age-matched controls (n=26, male=5; mean age 69.5±10.3 years, median age 68 years) were

analysed using flow cytometry in accordance with ethics approval (Belberry application number HREC 2011-10-497, Newcastle, New South Wales 2018/00207 and the University of Western Australia RA/4/20/5342). Fibrotic lung tissue was obtained from patients undergoing surgical lung biopsy or transplant surgery. All tissue was obtained with appropriate informed consent and its use approved by the East Midlands – Nottingham 2 NRES Committee (ref. no. 12/EM/0058).

Statistical analysis

Experiments with two sample groups were analysed using an unpaired t-test or Mann–Whitney U-test if the differences between two independent samples are not normally distributed. Experiments with more than two groups were analysed using a one-way ANOVA with *post hoc* Tukey test for multiple comparisons. A p-value <0.05 was considered significant.

Results

B-cells aggregate in the lungs of Blm-treated mice

In order to assess how Blm triggers B-cell accumulation in the lung, we evaluated B-cell numbers in the lung and circulation of wt mice by immunohistochemistry and flow cytometry. Tissue sections were stained with Martius scarlet blue to demonstrate the extent of fibrosis, with collagen shown in blue. In addition, sections of lung tissue were stained with the pan-B-cell antibody B220, which binds to the CD45 receptor expressed on mature B-cells. Peripheral blood B-cells were stained and analysed by flow cytometry using additional cell surface markers CD19 and CD20, which are expressed by mature B-cells. We hypothesised that B-cell numbers would initially increase in the circulation and then accumulate within the lung tissue. Immunohistochemical analysis of sections of C57Bl/6J mouse lung tissue at the peak of fibrosis, 28 days after Blm treatment, demonstrated an accumulation of multiple $B220^+$ B cell foci (figure 1a iv, arrows, and viii) compared to saline-treated controls (figure 1a ii, vi). Flow cytometry did not show any significant difference in circulating $CD19^+$ B-cells in mice at either 7 days (figure 1b) or 28 days after Blm treatment (figure 1c). We expected to see an increase in B-cells in the lung from day 7 to 28; however, there was no significant change (figure 1b and c).

Blm-induced collagen deposition is refractory to anti-CD20-mediated ablation of mature B-cells

To determine if anti-CD20-mediated depletion of mature B-cells protected Blm-treated mice from fibrosis, wt mice received prophylactic treatment comprising two doses of anti-CD20 antibody or an isotype control IgG2a antibody 7 days before and 7 days after Blm treatment (figure 2). Flow cytometry demonstrated almost a complete depletion of circulating $CD19^+$ B-cells (CD19 is a pan-B-cell marker expressed on all B-cells), on day 7 (prior to the second anti-CD20 antibody dose) and 28 days post-Blm treatment (figure 2a). In addition, immunohistochemistry and flow cytometry showed a decrease in the number of $B220^+$ cells in sections of spleen tissue (figure 2b) and $CD19^+$ cells from dissociated lung tissue (figure 2c) of anti-CD20 antibody treated mice compared with mice treated with the IgG2a isotype control antibody. However, anti-CD20 treatment did not show any significant change in fibrosis as determined by µCT and HPLC-assessed collagen deposition compared to mice that received the isotype control (figures 2d–f). To determine if the timing of B-cell depletion influences the fibrotic response, anti-CD20 antibodies were administered on days 10 and 19 post-Blm treatment. However, there was still no change in fibrosis compared with control (figure 2g).

$CD138^+$ plasma cells and $CD5^+$ cells were increased in the circulation and lungs of Blm-treated mice

Anti-CD20 antibody-mediated B-cell ablation prior to Blm treatment was not sufficient to reduce fibrosis. Therefore, we examined the different B-cell populations in wt C57BL/6 mice in response to saline or Blm treatment alone using flow cytometry and immunohistochemistry and compared them with saline controls. In Blm-only treated mice, there was no change in the frequency of $CD19^+$ $CD38^+$ plasmablasts in blood or $CD19^+$ $CD138^+$ plasma B-cells in lung or $CD5^+$ $CD19^+$ B-cells within the circulation or lung at day 7 or 28 compared with saline control (figures 3a–d). However, immunostaining demonstrated the formation of aggregates of $B220^+$, $CD19^+$, $CD138^+$ and $CD3^+$ cells in Blm-treated mouse lung (figure 3e and f).

We then examined the lymphocyte subsets of wt mice treated with saline or Blm only or those that received Blm with anti-CD20 treatment or an isotype control. Anti-CD20 depletion prior to Blm markedly reduced the number of $B220^+$ cells within the lung (figure 4a) and significantly reduced the number of $CD19^+$ lymphocytes within the circulation (figure 4b) of mice 28 days post-Blm treatment. An increase in the proportion of $CD5^+$ cells was detected within the lungs of anti-CD20 antibody-treated mice (figure 4a). Subsequent flow cytometry analysis of dissociated lung tissue showed that was due to a significant increase in $CD5^+CD3^+$ T-cells, but not $CD5^+CD19^+$ B-cells, excluding the possibility of expansion of $CD5^+$ B1-cells in the lung (figure 4b). In addition, a significant increase in plasma cell number was detected in anti-CD20 antibody-treated mice compared to IgG2a control (figure 4c). These data suggest

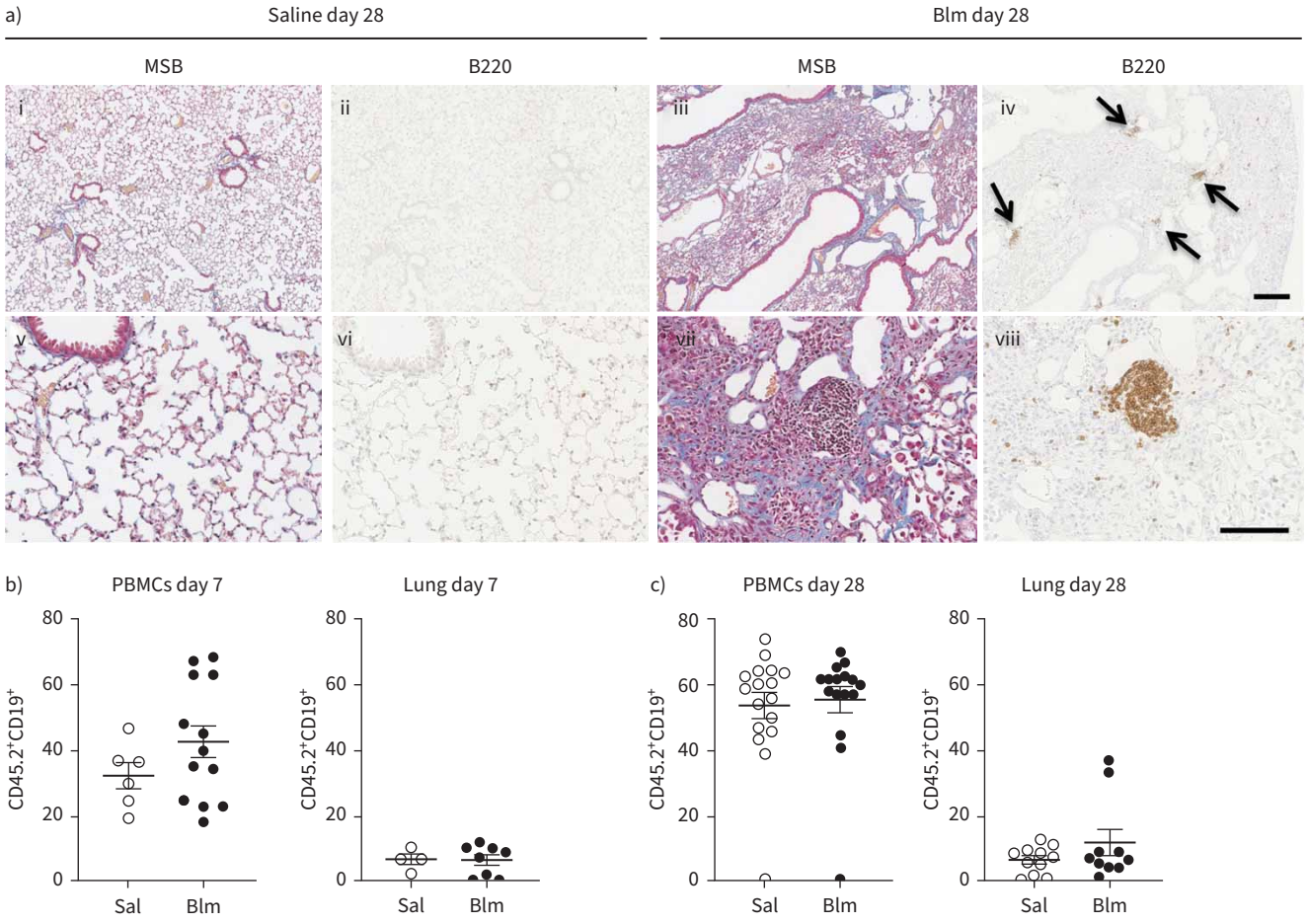

FIGURE 1 B-cells are a prominent feature in bleomycin (Blm)-induced pulmonary fibrosis in mice. a) Immunohistochemical analysis of B220 staining 28 days post-oropharyngeal Blm treatment reveals an increase in $B220^+$ cells (iv, arrows, and viii) at sites of fibrosis (Martius scarlet blue (MSB) staining, iii, vii collagen blue) compared to saline-treated controls (MSB i, v) and B220-stained (ii, vii). Images i–iv represent low magnification; scale bar=200 µm. Images v–iv represent high magnification; scale bar=100 µm. Images are representative of three mice in each group. b) Flow cytometry did not show a significant increase in circulating or lung resident $CD45.2^+$ $CD19^+$ B-cells in Blm-treated mice 7 days post-treatment ($n \geqslant 4$). c) No significant difference in circulating $CD45.2^+$ $CD19^+$ B-cells was detected in isolated peripheral blood mononuclear cells (PBMCs) 28 days following Blm treatment. There was no significant difference in the number of $CD19^+$ cells detected in dissociated lung tissue post-Blm treatment. Statistical analysis was performed using an unpaired t-test ($n \geqslant 10$).

that while prophylactic anti-CD20 depletion successfully targeted CD20 expressing B-cells, there were a large number of plasma cells that remained in the lung following Blm treatment and may have contributed to the lung fibrosis.

Plasma cell depletion inhibited lung fibrosis

To investigate a role for plasma cells in lung fibrosis, we treated Blm-exposed mice twice weekly with bortezomib, a selective inhibitor of the 26S proteasome that targets plasma cells and is used for the treatment of multiple myeloma and mantle-cell lymphoma. Mice treated with bortezomib showed a significant reduction in fibrosis as determined by µCT analysis (figure 5a). Immunfluorescent staining of the lungs for CD138 expression showed almost complete absence of plasma cells in bortezomib-treated lungs (figure 5b).

B-cell accumulation in IPF

We then explored to what extent the mouse data corroborated with clinical data of B-cell accumulation in lung sections from IPF patients. Immunohistochemistry performed on IPF lung tissue showed an accumulation of $CD20^+$, $CD5^+$ and $CD138^+$ cells within regions of fibrosis (figure 6a), consistent with observations in the lungs of Blm-treated mice. The peripheral blood of IPF patients also contained a

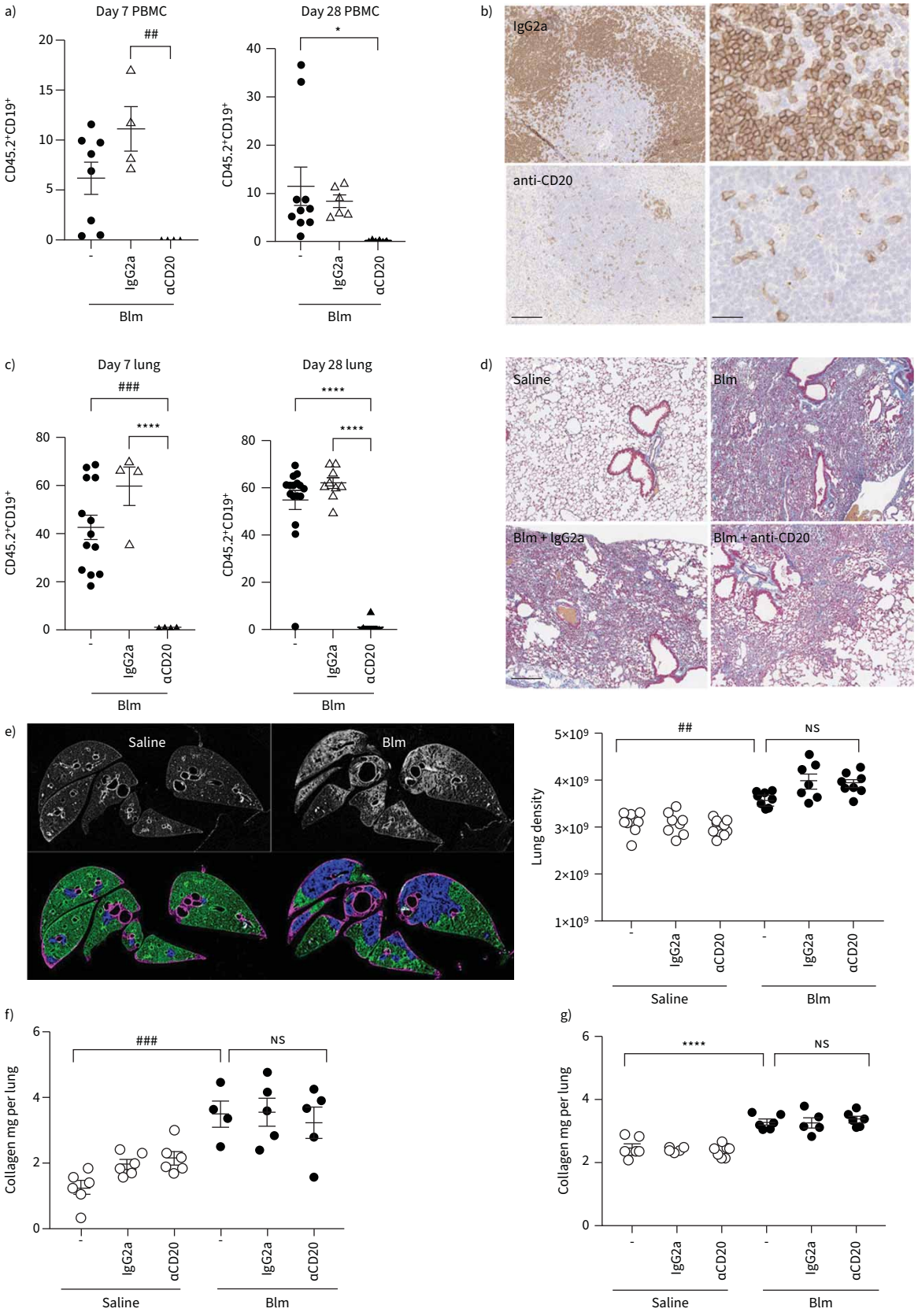

FIGURE 2 Anti-CD20-mediated B-cell depletion does not protect mice against oropharyngeal bleomycin (Blm)-induced pulmonary fibrosis. a) Anti-CD20 therapy 7 days prior to and 7 days following Blm successfully reduced circulating $CD19^+$ cells as measured by flow cytometry in mice

on day 7 and 28 post Blm treatment (n⩾4). b) Immunohistochemical analysis of B220 expression on spleen tissue sections demonstrated a marked decrease in $B220^+$ cell numbers in anti-CD20-treated mice compared to IgG2a-treated control mice. Scale bars=100 µm (25 µm higher power). c) Quantitative flow cytometry analysis showed that anti-CD20 treatment significantly reduced Blm-induced $CD19^+$ cell numbers in the lung on day 7 and day 28 (n⩾4). d) Masson's trichrome staining showed no overt difference in the extent of collagen deposition (blue) in mice treated with Blm and anti-CD20 compared to Blm only and mice treated with Blm and IgG2a. Scale bars=200 µm. e–g) Quantitative analysis of fibrosis and collagen deposition was performed using micro computed tomography (µCT) and high-performance liquid chromatography (HPLC) analysis of hydroxyproline, but there was no significant difference in mice treated with Blm and anti-CD20 compared with Blm and vehicle control. e) Represents a preventative model where anti-CD20 was administered 7 days prior to, and 7 days after Blm treatment. µCT analysis was performed *ex vivo* and the lung density was used as a representation of fibrosis. There was no difference in the amount of Blm-induced fibrosis in IgG2a or αCD20 treated mice (n⩾7). f) HPLC analysis did not show any difference in the amount of Blm-induced lung collagen in in IgG2a- or αCD20-treated mice, confirming that αCD20 had no effect on lung fibrosis (n⩾6). g) The data represent a therapeutic model where anti-CD20 was administered on days 10 and 19 post-Blm treatment. Similarly, there was no detectable change in the amount of collagen in the lungs of Blm and anti-CD20 treated mice compared to Blm alone or Blm- and IgG2a-treated mice (HPLC n⩾5 and µCT n⩾6). All images are representative of at least three mice per group. *: p⩽0.05, ##: p⩽0.005, ###: p⩽0.0005, ****: p⩽0.0001.

significant increase in plasmablasts compared with healthy controls (figure 6b). To determine if plasmablast numbers are maintained in IPF patients, four surviving IPF patients were re-bled 18 months after their initial blood sample and plasmablast numbers assessed using flow cytometry. All four surviving IPF patients demonstrated an even higher proportion of plasmablasts in their blood compared to the primary bleed (figure 5c and d).

Discussion

There is growing evidence that the immune system plays an important role in the pathobiology of a range of fibrotic diseases including IPF, SSc and liver fibrosis [4]. Using a mouse model of Blm-induced lung fibrosis, we demonstrated previously that B-cells were an important effector cell population in the regulation of lung fibrosis in mice [30]. Genetic depletion of *Rag1* on a high STAT3 background blocked the formation of mature B- and T-cells and this was sufficient to protect the lungs of mice from Blm-induced fibrosis. Furthermore, genetic depletion of mature B-cells in $muMt^{-/-}$ mice on a high STAT3 background and $CD19^{-/-}$ mice, which have reduced B-cell activation, also reduced collagen synthesis and fibrosis following Blm treatment, specifically implicating mature B-cells in lung fibrogenesis [30, 34]. Yet, an important question remained as to the identity of the B-cell subset that might contribute to fibrotic disease.

To assess the implication of these genetic findings, we explored a more clinically relevant model of B-cell depletion; mouse anti-CD20 antibody treatment, based on the human anti-CD20 antibody, rituximab. Here we reveal that antibody-mediated depletion of $CD20^+$ B-cells, which successfully removed ∼95% of mature B-cells from the peripheral circulation and tissues [35], did not prevent Blm-induced lung fibrosis. To resolve this discrepancy, we firstly demonstrated that antibody-mediated B-cell depletion failed to remove all mature B-cell populations. Plasma cells downregulate CD20 during their differentiation making them resistant to anti-CD20 antibody depletion, allowing their retention in the blood and peripheral tissues. However, plasma cells have been implicated in autoimmune diseases such as SLE, vasculitis and Sjogren syndrome through the production of self-reactive antibodies to either host proteins or nucleic acids [19, 36].

Several studies have shown that IPF patients have increased plasmablasts compared to controls [4, 37, 38]. Furthermore, proteomic analysis on IPF lung tissue demonstrated an accumulation of MZB-1-positive B-cells that were characterised as $CD20^-CD138^+CD38^+CD27^+$ [39], which share a number of phenotypic properties with conventional plasma cells. Groot Kormelink *et al.* [40] also showed that plasma cells and activated mast cells accumulate in the lung tissue of patients with IPF and hypersensitivity pneumonitis. Interestingly, one study using single-cell RNA-sequencing data did not show a significant increase in plasma cells or plasmablasts in IPF, but it was unclear what criteria were used to categorise these cells [41]. In this study we confirmed the presence of plasma cells and plasmablasts in the lung and blood, respectively, of IPF patients, and showed that plasmablasts were increased in a subpopulation of IPF patients compared with controls, consistent with other studies.

Plasmablasts are plasma cell precursors derived from the differentiation of activated memory B-cells generated in response to antigen exposure. Plasmablasts are short-lived antibody-secreting effector cells in the immune system and exhibit a transient presence in the peripheral blood during their transit from secondary lymphoid tissues (*e.g.* lymph node or spleen) to the bone marrow, where they can give rise to long-lived plasma cells. Currently there is little known about the origin and persistence of B-cell subsets in

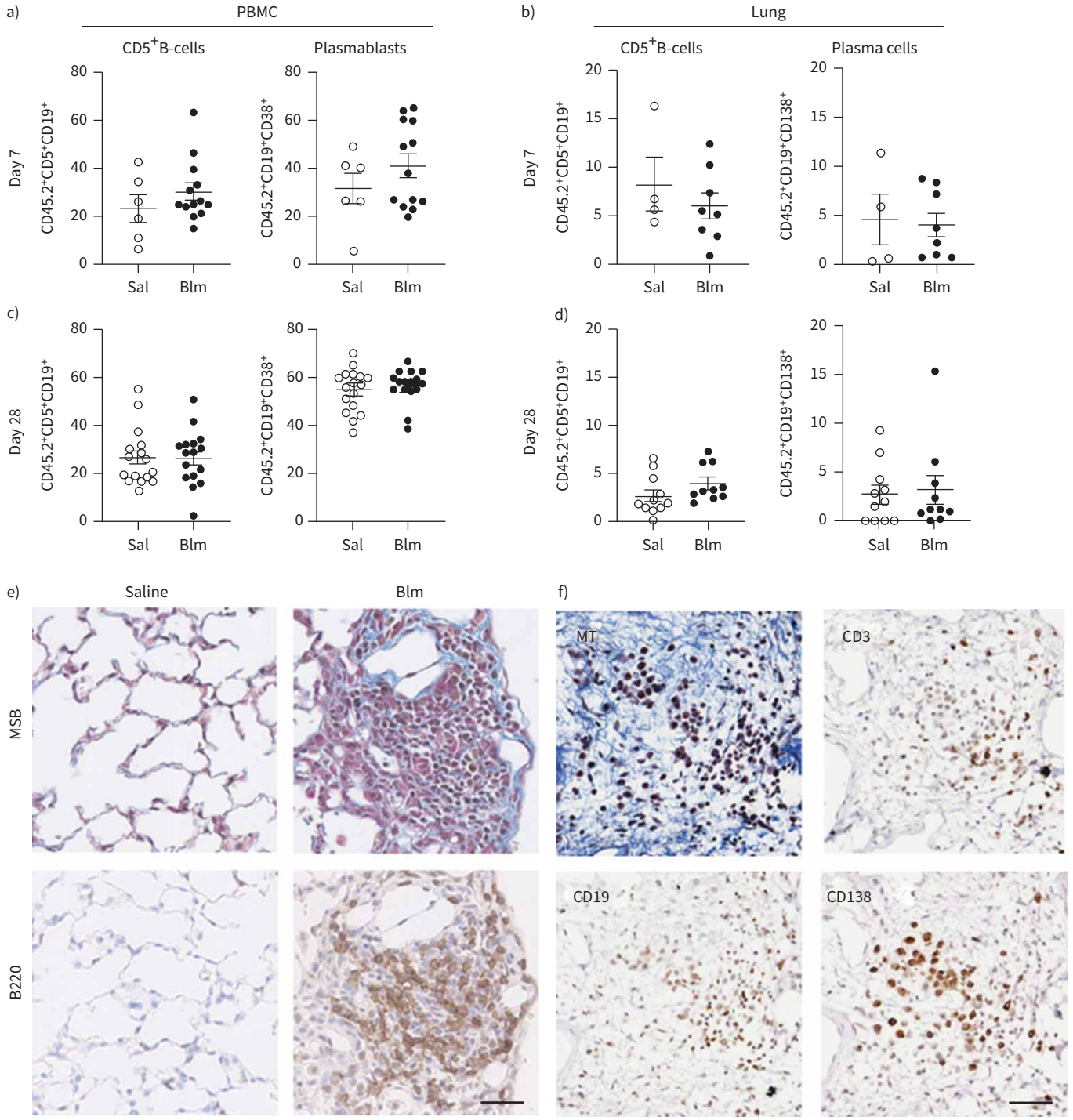

FIGURE 3 Characterisation of specific B-cell subsets in the peripheral circulation and lung of mice following oropharyngeal bleomycin (Blm)-induced pulmonary fibrosis. a) Blm treatment had no effect on the number of $CD5^+CD19^+$ B-cells or $CD19^+CD38^+CD138^+$ plasma cells detected in peripheral blood mononuclear cells (PBMCs) on day 7 post-Blm treatment ($n \geqslant 6$) or b) $CD5^+CD19^+$ B-cells or $CD19^+CD138^+$ PCs in the lung 7 days post-Blm treatment ($n \geqslant 4$). c, d) No significant difference was observed in the frequency of $CD19^+CD138^+$ plasma cells in the circulation or the lung at day 28 post-Blm treatment ($n \geqslant 6$). No significant increase in $CD5^+CD19^+$ cells was observed in the lung 28 days post-Blm treatment ($n \geqslant 6$). Statistical analysis was performed using an unpaired t-test. e) Mouse lung tissue from saline-treated or Blm-treated mice (day 28) was stained with Martius scarlet blue (MSB; collagen blue) or with anti-B220 antibody. $B220^+$ cell aggregates were detected in the lungs of Blm-treated mice (brown 3,3′-diaminobenzidine staining). f) Serial sections of Blm-treated lung stained with Masson's trichrome (MT) and immune markers. $CD3^+$ lymphocytes, $CD19^+$ B-cells and $CD138^+$ plasma cells were detected at sites of fibrosis. All images are representative of at least three mice per group. Scale bars=50 µm.

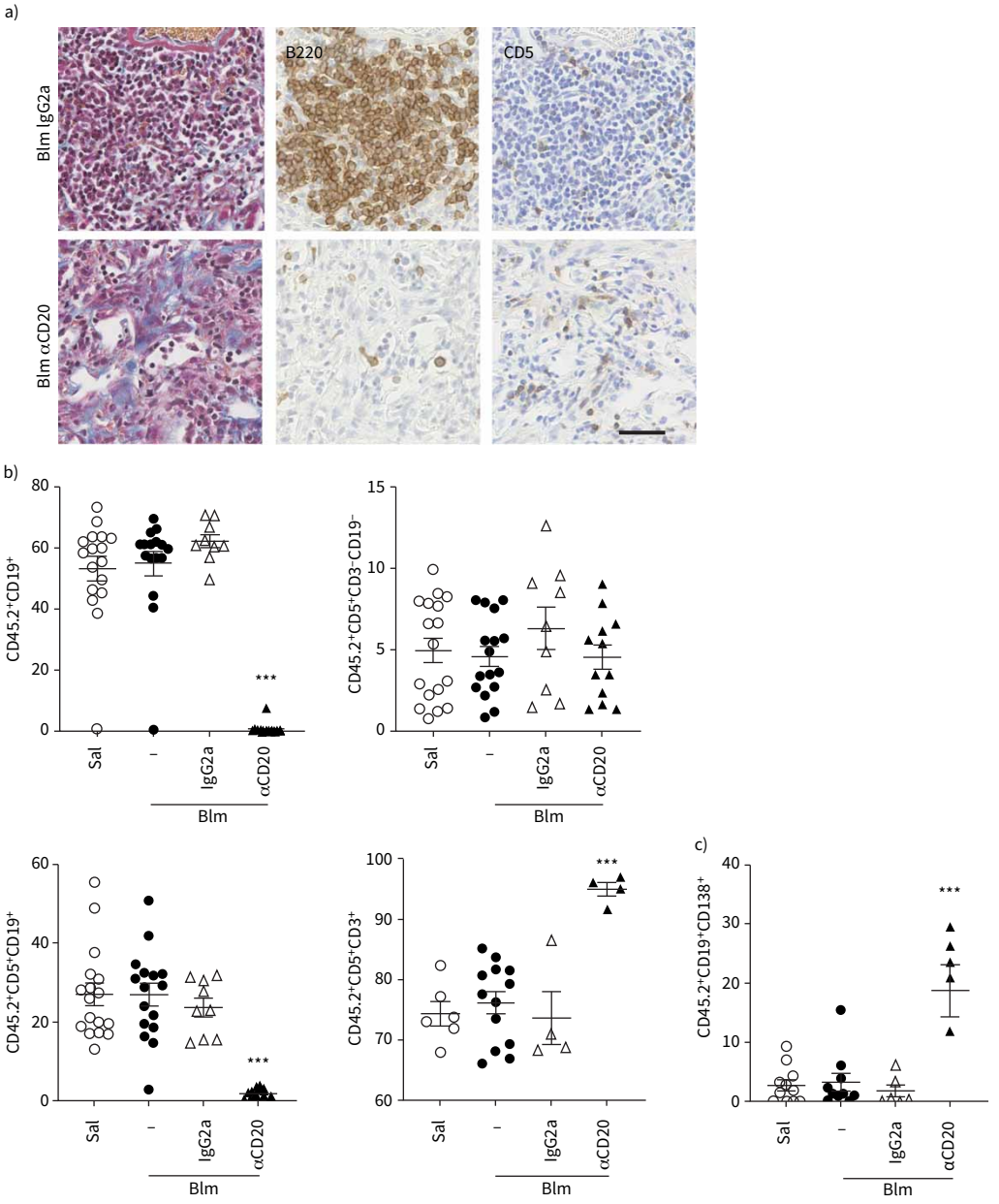

FIGURE 4 B-cell composition of the lungs of mice following anti-CD20 and bleomycin (Blm) treatment. a) Mouse lung tissue from Blm-exposed mice treated with anti-CD20 or isotype control (day 28) was stained with Masson's trichrome (collagen blue). Immunohistochemistry shows a marked reduction in $B220^+$ B-cells in 28-day treated mice and retention of $CD5^+$ expressing cells compared with mice treated with Blm and IgG2a. All images are representative of at least three mice per group. Scale bars=50 µm. b) Flow cytometry confirms depletion of $CD19^+$ cells in the circulation, but revealed no increase in circulating $CD5^+$ B-cells, but a significant increase in $CD5^+$ T-cells following anti-CD20 depletion ($n \geqslant 4$). c) However, anti-CD20 treatment did not deplete the plasma cell population in the lung 28 days following Blm ($n \geqslant 5$). NS: nonsignificant. Statistical analysis was performed using one-way ANOVA. ***: $p \leqslant 0.001$.

IPF patients. To begin to address this issue, we re-bled four surviving IPF patients 18 months after their initial blood sample and the second sample was analysed using flow cytometry. All four IPF patients displayed even higher proportion of plasmablasts in the blood compared to the primary bleed, suggesting that these patients must experience ongoing immune responses that could be in response to exposure to environmental antigens or self-antigens.

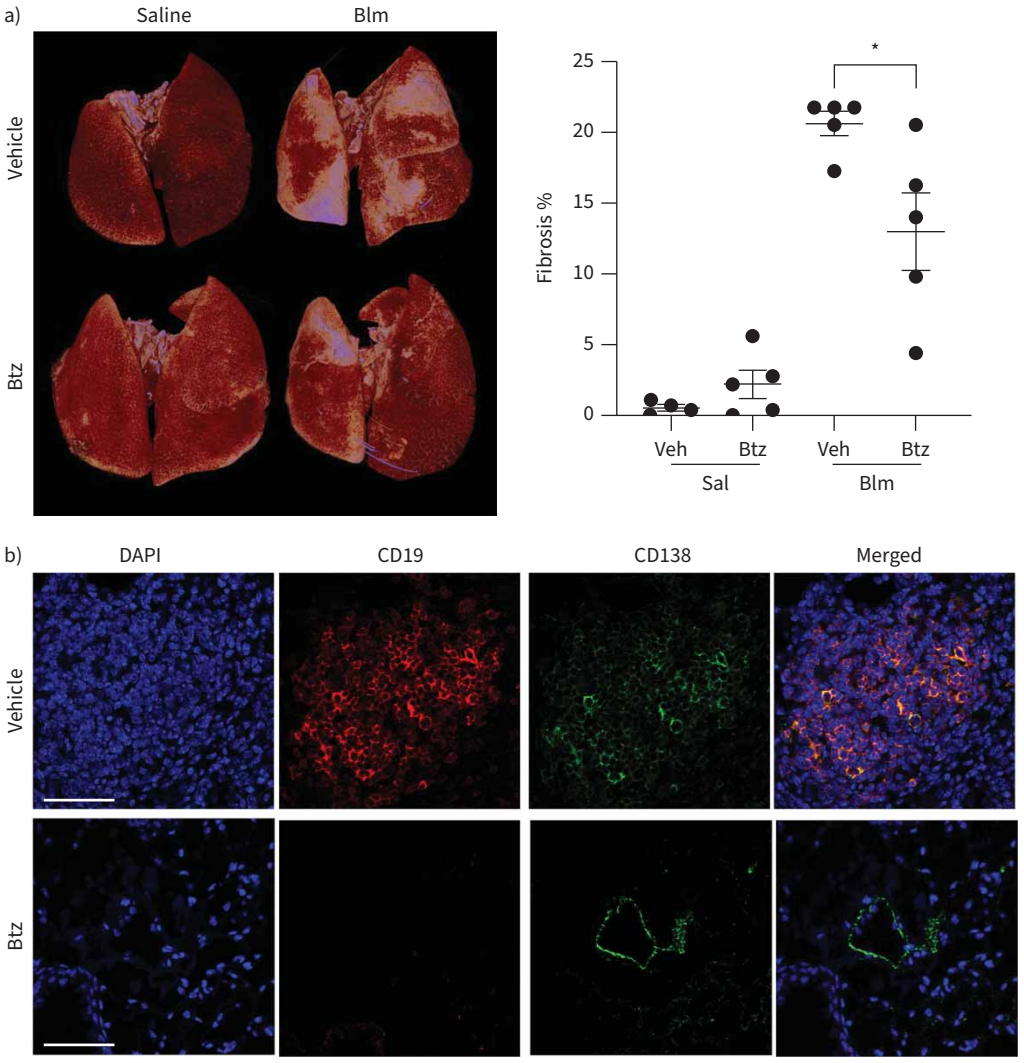

FIGURE 5 Plasma cell depletion reduces bleomycin (Blm)-induced lung fibrosis. Mice were given either a vehicle control or bortezomib (Btz) at day −7 and twice weekly until 28 days after intranasal Blm (2 mg·kg^{-1}) treatment (day 0) and the volume of fibrosis was quantified by micro-computed tomography analysis. a) Blm induced significant lung fibrosis compared to saline, which was reduced following bortezomib treatment (n⩾4). b) Immunofluorescence staining of lung tissue from Blm+vehicle or bortezomib-treated mice was performed to detect plasma cells within the lungs. The nuclei are stained blue, CD19^{+} cells are stained red and CD138^{+} cells are stained green. The plasma cells are positive for both CD19 and CD138. Some epithelial cell staining is seen in the bortezomib-treated group. The figure shows a representative image from each group (n⩾4). Scale bars=60 μm. DAPI: 4′,6-diamidino-2-phenylindole. *: p<0.05. A lower-power image showing an extensive area of fibrosis is shown in supplementary figure S3.

Rituximab is a human anti-CD20 antibody that has been used clinically to deplete B-cells in autoimmune diseases and different types of haematological cancers [42–44]. Rituximab has also been used in clinical trials for SSc, non-IPF ILDs and IPF exacerbations [45–47] with mixed results and limited improvement in lung function. Rituximab reduced recall responses to some antigens in lymphoma and rheumatoid arthritis patients, but total immunoglobulin (Ig) levels in patients remained unchanged [48]. Therefore, if plasma cells have a role in the pathobiology of IPF, the use of rituximab for immunotherapy may be limited. DiLillo *et al.* [43] revealed that anti-CD20 antibody treatment in wt mice depleted natural and antigen-induced IgM responses and memory B-cell populations, but had no effect on the number of long-lived plasma cells in bone marrow, nor the total serum Ig levels or the titres of antigen-specific antibodies. Treatment of adult autoimmune tight skin mice, a genetic model of SSc, with anti-CD20, did not affect skin fibrosis or autoantibody levels with established disease; however, continuous delivery of anti-CD20 to young neonatal

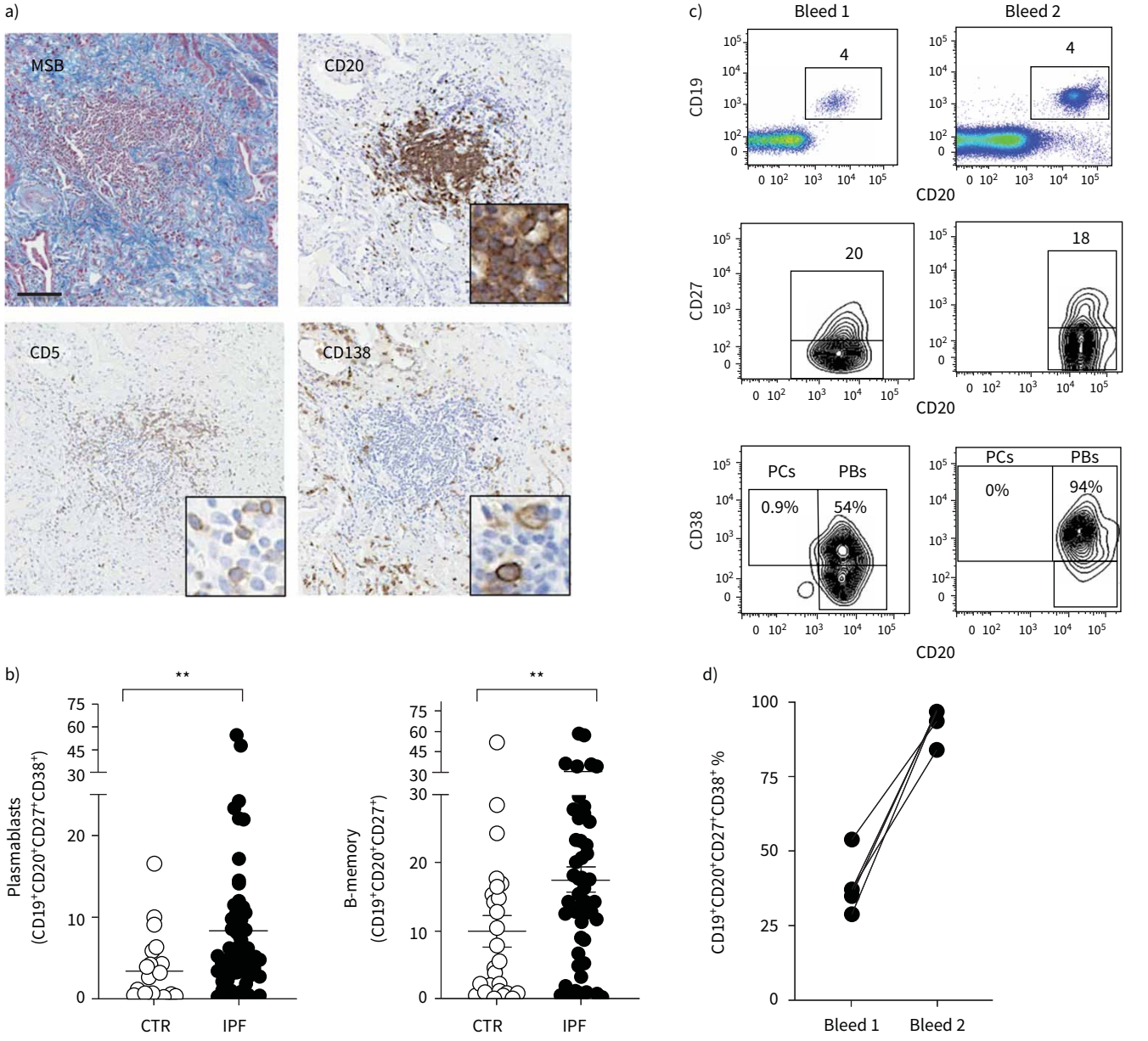

FIGURE 6 Analysis of B-cell populations in the lung and peripheral blood of idiopathic pulmonary fibrosis (IPF) patients and aged matched healthy controls (CTR). a) Martius scarlet blue (MSB) stained and anti-CD20 stained sections of IPF lung tissue demonstrate collagen deposition (blue) and an accumulation of $CD20^+$ B-cells within regions of fibrosis (brown). In addition, $CD5^+$ and $CD138^+$ plasma cells were abundant in IPF lung tissue. All images are representative of at least three mice per group. Scale bars=50 µm. b) Quantitation of the frequency of plasmablasts and memory B-cells in white blood cells of healthy controls (n=27) and IPF patients (n=51) as determined by flow cytometry. Each symbol represents the value from one individual. c) Representative dot plot and contour plots of $CD19^+$ $CD20^+$ B-cells from an IPF patient who was bled on two separate occasions 18 months apart. $CD19^+$ *versus* $CD20^+$ staining identifies mature B-cells (top), $CD20^+CD27^+$ cells identifies memory B-cells (middle) and $CD20^+$ $CD38^+$ identifies plasmablasts (PBs) (bottom), n=4. d) Frequency of $CD19^+CD20^+$ $CD27^+$ $CD38^+$ plasmablasts in the peripheral blood of four different individuals bled on two occasions 18 months apart. PCs: plasma cells.

tight skin mice prior to disease onset reduced skin fibrosis and autoantibody production [35]. Plasma cells are resistant to elimination by the anti-CD20 antibody because they lack expression of the target antigen. Therefore, plasma cell targeted therapies are required to treat autoimmune diseases or cancers like multiple myeloma, a leukaemia of plasma cells. Monoclonal antibody therapies are currently used in clinical practice to target other plasma cell surface markers including signalling lymphocyte activation molecule F7 (SlamF7)

and CD38 [49, 50], while the proteasome inhibitor bortezomib is an anticancer therapy used in the treatment of multiple myeloma, but toxicity and off-target effects are common [51].

The function of the proteasome is critically important in plasma cells because of their high rate of antibody synthesis. Proteasome inhibition in plasma cells causes accumulation of defective immunoglobulins and misfolded proteins, resulting in plasma cell death [52–54]. Proteosome inhibitors have been shown to ameliorate symptoms in patients with autoimmune diseases including SLE, rheumatoid arthritis, myasthenia gravis, neuromyelitis optica spectrum disorder, chronic inflammatory demyelinating polyneuropathy and autoimmune haematological diseases that were unresponsive to conventional therapies [55]. Bortezomib has been shown to significantly reduce lung fibrosis in Blm-treated mice in two other studies, although it was suggested that its effects were through inhibition of transforming growth factor-β signalling [56] or by modulating fibroblast function independent of proteasome inhibition [57]. In this study we confirmed that bortezomib reduced lung fibrosis in Blm-treated mice, but also showed almost complete depletion of plasma cells in bortezomib-treated lung tissue. Although we cannot conclude that the effects of bortezomib are solely due to plasma cell depletion, the observation that genetic depletion of mature B-cells in $Rag^{-/-}$and $muMT^{-/-}$ mice [30] and reduced B-cell activation in $CD19^{-/-}$ mice, which all inhibit plasma cell function, block Blm-induced lung fibrosis, yet CD20 depletion which does not inhibit plasma cell function doesn't inhibit fibrosis, strongly supports a role for plasma cells in the development of lung fibrosis.

In conclusion, this study provides new evidence supporting the role of plasma cells and plasmablasts in Blm-induced lung fibrosis, and importantly, for their accumulation in the lungs of clinically diagnosed IPF patients. The results presented here have important implications in our understanding of B-cell subsets in pulmonary fibrosis and for the consideration of future therapies in IPF. It will be important to determine whether there is clonal expansion of particular plasma cells and to identify antigen specificity of antibodies produced by plasma cells in IPF patients to elucidate their role in tissue damage and whether they are directed to self or foreign antigens. Resolving these issues may help guide the development and use of immune therapies in IPF.

Acknowledgements: The authors would like to acknowledge the generosity of Genentech (USA) for providing the anti-CD20 used in this study. In addition, we would like to thank Chuan Bian Lim (Institute for Respiratory Health, Nedlands, Australia) and Joe Yasa (Murdoch University, Murdoch, Australia) for technical support and the Institute for Respiratory Health's Clinical Trial Unit for blood sample collection. We acknowledge the facilities and the scientific and technical assistance of the Australian Microscopy and Microanalysis Research Facility at the Centre for Microscopy, Characterisation and Analysis, University of Western Australia, a facility funded by the University, State and Commonwealth Governments.

Conflict of interest: S.E. Mutsaers, C.M. Prêle, R.J. McAnulty, G.J. Laurent, G. Hoyne, D.A. Knight, R.J. O'Donoghue and M. Ernst received grants from National Health and Medical Research Council (NHMRC), project grants ID APP1067511. R.J. McAnulty, S.E. Mutsaers, C.M. Prêle and D.R. Pearce received grants from British Lung Foundation, project grant number PPRG15-10. T. Miles reports that Genentech provided the anti-CD20 antibody, and received UWA Research Training Program Scholarship and the Lung Foundation Australia Bill van Nierop PhD Scholarship. All other authors have nothing to disclose.

Support statement: This work is funded by National Health and Medical Research Council (NHMRC) project grant #1067511 and British Lung Foundation Grant PPRG15-10. C.M. Prêle, M. Fear and S.E. Mutsaers are supported by NHMRC project grant #1127337. T. Miles is supported by a University of Western Australia Research Training Postgraduate Award and the Lung Foundation Australia Bill van Nierop PhD Scholarship. Funding information for this article has been deposited with the Crossref Funder Registry.

References

1 Lederer DJ, Martinez FJ. Idiopathic pulmonary fibrosis. *N Engl J Med* 2018; 378: 1811–1823.
2 Maher TM, Evans IC, Bottoms SE, *et al.* Diminished prostaglandin E2 contributes to the apoptosis paradox in idiopathic pulmonary fibrosis. *Am J Respir Crit Care Med* 2010; 182: 73–82.
3 Richeldi L, Collard HR, Jones MG. Idiopathic pulmonary fibrosis. *Lancet* 2017; 389: 1941–1952.
4 Heukels P, van Hulst JAC, van Nimwegen M, *et al.* Enhanced Bruton's tyrosine kinase in B-cells and autoreactive IgA in patients with idiopathic pulmonary fibrosis. *Respir Res* 2019; 20: 232.
5 Hoyne GF, Elliott H, Mutsaers SE, *et al.* Idiopathic pulmonary fibrosis and a role for autoimmunity. *Immunol Cell Biol* 2017; 95: 577–583.
6 Marchal-Sommé J, Uzunhan Y, Marchand-Adam S, *et al.* Cutting edge: nonproliferating mature immune cells form a novel type of organized lymphoid structure in idiopathic pulmonary fibrosis. *J Immunol* 2006; 176: 5735–5739.

7 Todd NW, Scheraga RG, Galvin JR, *et al.* Lymphocyte aggregates persist and accumulate in the lungs of patients with idiopathic pulmonary fibrosis. *J Inflamm Res* 2013; 6: 63–70.
8 Dobashi N, Fujita J, Murota M, *et al.* Elevation of anti-cytokeratin 18 antibody and circulating cytokeratin 18: anti-cytokeratin 18 antibody immune complexes in sera of patients with idiopathic pulmonary fibrosis. *Lung* 2000; 178: 171–179.
9 Rioja I, Hughes FJ, Sharp CH, *et al.* Potential novel biomarkers of disease activity in rheumatoid arthritis patients: CXCL13, CCL23, transforming growth factor α, tumor necrosis factor receptor superfamily member 9, and macrophage colony-stimulating factor. *Arthritis Rheum* 2008; 58: 2257–2267.
10 Shum AK, Alimohammadi M, Tan CL, *et al.* BPIFB1 is a lung-specific autoantigen associated with interstitial lung disease. *Sci Transl Med* 2013; 5: 206ra139.
11 Shum AK, DeVoss J, Tan CL, *et al.* Identification of an autoantigen demonstrates a link between interstitial lung disease and a defect in central tolerance. *Sci Transl Med* 2009; 1: 9ra20.
12 Fischer A, du Bois R. Interstitial lung disease in connective tissue disorders. *Lancet* 2012; 380: 689–698.
13 Jonsson MV, Skarstein K, Jonsson R, *et al.* Serological implications of germinal center-like structures in primary Sjögren's syndrome. *J Rheumatol* 2007; 34: 2044–2049.
14 Kogame T, Yamashita R, Hirata M, *et al.* Analysis of possible structures of inducible skin-associated lymphoid tissue in lupus erythematosus profundus. *J Dermatol* 2018; 45: 1117–1121.
15 Takemura S, Braun A, Crowson C, *et al.* Lymphoid neogenesis in rheumatoid synovitis. *J Immunol* 2001; 167: 1072–1080.
16 Wallace WA, Howie SE. Upregulation of tenascin and TGFβ production in a type II alveolar epithelial cell line by antibody against a pulmonary auto-antigen. *J Pathol* 2001; 195: 251–256.
17 Wallace WA, Roberts SN, Caldwell H, *et al.* Circulating antibodies to lung protein(s) in patients with cryptogenic fibrosing alveolitis. *Thorax* 1994; 49: 218–224.
18 Cremasco V, Woodruff MC, Onder L, *et al.* B cell homeostasis and follicle confines are governed by fibroblastic reticular cells. *Nat Immunol* 2014; 15: 973–981.
19 Hiepe F, Radbruch A. Plasma cells as an innovative target in autoimmune disease with renal manifestations. *Nat Rev Nephrol* 2016; 12: 232–240.
20 Shapiro-Shelef M, Calame K. Regulation of plasma-cell development. *Nat Rev Immunol* 2005; 5: 230–242.
21 Ionescu L, Urschel S. Memory B cells and long-lived plasma cells. *Transplantation* 2019; 103: 890–898.
22 Nutt SL, Hodgkin PD, Tarlinton DM, *et al.* The generation of antibody-secreting plasma cells. *Nat Rev Immunol* 2015; 15: 160–171.
23 de Vinuesa CG, Cook MC, Ball J, *et al.* Germinal centers without T cells. *J Exp Med* 2000; 191: 485–494.
24 Sze DM, Toellner KM, García de Vinuesa C, *et al.* Intrinsic constraint on plasmablast growth and extrinsic limits of plasma cell survival. *J Exp Med* 2000; 192: 813–821.
25 Berland R, Wortis HH. Origins and functions of B-1 cells with notes on the role of CD5. *Annu Rev Immunol* 2002; 20: 253–300.
26 Ehrenstein MR, Notley CA. The importance of natural IgM: scavenger, protector and regulator. *Nat Rev Immunol* 2010; 10: 778–786.
27 Casciola-Rosen LA, Anhalt G, Rosen A. Autoantigens targeted in systemic lupus erythematosus are clustered in two populations of surface structures on apoptotic keratinocytes. *J Exp Med* 1994; 179: 1317–1330.
28 Peng Y, Kowalewski R, Kim S, *et al.* The role of IgM antibodies in the recognition and clearance of apoptotic cells. *Mol Immunol* 2005; 42: 781–787.
29 Halle S, Dujardin HC, Bakocevic N, *et al.* Induced bronchus-associated lymphoid tissue serves as a general priming site for T cells and is maintained by dendritic cells. *J Exp Med* 2009; 206: 2593–2601.
30 O'Donoghue RJ, Knight DA, Richards CD, *et al.* Genetic partitioning of interleukin-6 signalling in mice dissociates Stat3 from Smad3-mediated lung fibrosis. *EMBO Mol Med* 2012; 4: 939–951.
31 Prêle CM, Yao E, O'Donoghue RJ, *et al.* STAT3: a central mediator of pulmonary fibrosis? *Proc Am Thorac Soc* 2012; 9: 177–182.
32 Scotton CJ, Hayes B, Alexander R, *et al. Ex vivo* micro-computed tomography analysis of bleomycin-induced lung fibrosis for preclinical drug evaluation. *Eur Respir J* 2013; 42: 1633–1645.
33 Mutsaers SE, Foster ML, Chambers RC, *et al.* Increased endothelin-1 and its localization during the development of bleomycin-induced pulmonary fibrosis in rats. *Am J Respir Cell Mol Biol* 1998; 18: 611–619.
34 Komura K, Yanaba K, Horikawa M, *et al.* CD19 regulates the development of bleomycin-induced pulmonary fibrosis in a mouse model. *Arthritis Rheum* 2008; 58: 3574–3584.
35 Hasegawa M, Hamaguchi Y, Yanaba K, *et al.* B-lymphocyte depletion reduces skin fibrosis and autoimmunity in the tight-skin mouse model for systemic sclerosis. *Am J Pathol* 2006; 169: 954–966.
36 Chesi M, Bergsagel PL. Molecular pathogenesis of multiple myeloma: basic and clinical updates. *Int J Hematol* 2013; 97: 313–323.
37 Li X, Huang Y, Ye N, *et al.* Analysis of immune-related genes in idiopathic pulmonary fibrosis based on bioinformatics and experimental verification. *Ann Palliat Med* 2021; 10: 11598–11614.

38 Xue J, Kass DJ, Bon J, *et al.* Plasma B lymphocyte stimulator and B cell differentiation in idiopathic pulmonary fibrosis patients. *J Immunol* 2013; 191: 2089–2095.

39 Schiller HB, Mayr CH, Leuschner G, *et al.* Deep proteome profiling reveals common prevalence of MZB1-positive plasma B cells in human lung and skin fibrosis. *Am J Respir Crit Care Med* 2017; 196: 1298–1310.

40 Groot Kormelink T, Pardo A, Knipping K, *et al.* Immunoglobulin free light chains are increased in hypersensitivity pneumonitis and idiopathic pulmonary fibrosis. *PLoS One* 2011; 6: e25392.

41 Adams TS, Schupp JC, Poli S, *et al.* Single-cell RNA-seq reveals ectopic and aberrant lung-resident cell populations in idiopathic pulmonary fibrosis. *Sci Adv* 2020; 6: eaba1983.

42 Colombat P, Salles G, Brousse N, *et al.* Rituximab (anti-CD20 monoclonal antibody) as single first-line therapy for patients with follicular lymphoma with a low tumor burden: clinical and molecular evaluation. *Blood* 2001; 97: 101–106.

43 DiLillo DJ, Hamaguchi Y, Ueda Y, *et al.* Maintenance of long-lived plasma cells and serological memory despite mature and memory B cell depletion during CD20 immunotherapy in mice. *J Immunol* 2008; 180: 361–371.

44 Reff ME, Carner K, Chambers KS, *et al.* Depletion of B cells *in vivo* by a chimeric mouse human monoclonal antibody to CD20. *Blood* 1994; 83: 435–445.

45 Daoussis D, Melissaropoulos K, Sakellaropoulos G, *et al.* A multicenter, open-label, comparative study of B-cell depletion therapy with rituximab for systemic sclerosis-associated interstitial lung disease. *Semin Arthritis Rheum* 2017; 46: 625–631.

46 Donahoe M, Valentine VG, Chien N, *et al.* Autoantibody-targeted treatments for acute exacerbations of idiopathic pulmonary fibrosis. *PLoS One* 2015; 10: e0127771.

47 Elhai M, Boubaya M, Distler O, *et al.* Outcomes of patients with systemic sclerosis treated with rituximab in contemporary practice: a prospective cohort study. *Ann Rheum Dis* 2019; 78: 979–987.

48 Cambridge G, Leandro MJ, Edwards JC, *et al.* Serologic changes following B lymphocyte depletion therapy for rheumatoid arthritis. *Arthritis Rheum* 2003; 48: 2146–2154.

49 de Weers M, Tai YT, van der Veer MS, *et al.* Daratumumab, a novel therapeutic human CD38 monoclonal antibody, induces killing of multiple myeloma and other hematological tumors. *J Immunol* 2011; 186: 1840–1848.

50 Tai YT, Dillon M, Song W, *et al.* Anti-CS1 humanized monoclonal antibody HuLuc63 inhibits myeloma cell adhesion and induces antibody-dependent cellular cytotoxicity in the bone marrow milieu. *Blood* 2008; 112: 1329–1337.

51 Loke C, Mollee P, McPherson I, *et al.* Bortezomib use and outcomes for the treatment of multiple myeloma. *Intern Med J* 2020; 50: 1059–1066.

52 Field-Smith A, Morgan GJ, Davies FE. Bortezomib (Velcade^{TM}) in the treatment of multiple myeloma. *Ther Clin Risk Manag* 2006; 2: 271–279.

53 Obeng EA, Carlson LM, Gutman DM, *et al.* Proteasome inhibitors induce a terminal unfolded protein response in multiple myeloma cells. *Blood* 2006; 107: 4907–4916.

54 Wang J, Fang Y, Fan RA, *et al.* Proteasome inhibitors and their pharmacokinetics, pharmacodynamics, and metabolism. *Int J Mol Sci* 2021; 22: 11595.

55 Khalesi N, Korani S, Korani M, *et al.* Bortezomib: a proteasome inhibitor for the treatment of autoimmune diseases. *Inflammopharmacology* 2021; 29: 1291–1306.

56 Mutlu GM, Budinger GR, Wu M, *et al.* Proteasomal inhibition after injury prevents fibrosis by modulating TGF-β_1 signalling. *Thorax* 2012; 67: 139–146.

57 Penke LRK, Speth J, Wettlaufer S, *et al.* Bortezomib inhibits lung fibrosis and fibroblast activation without proteasome inhibition. *Am J Respir Cell Mol Biol* 2022; 66: 23–37.